Available online at www.sciencedirect.com
SCIENCE DIRECT
Polymer 47 (2006) 67–74
polymer
www.elsevier.com/locate/polymer

High resolution solution and solid state NMR characterization of ethylene/1-butene and ethylene/1-hexene copolymers fractionated by preparative temperature rising elution fractionation

H.J. Assumption [a], J.P. Vermeulen [c], W.L. Jarrett [b], L.J. Mathias [b], A.J. van Reenen [c,*]

[a] Sasol Technology R&D, P.O. Box 1, Sasolburg 1947, South Africa
[b] Department of Polymer Science, University of Southern Mississippi, 118 College Drive #10076, Hattiesburg, MS 39406-0076, USA
[c] Department of Chemistry and Polymer Science, University of Stellenbosch, P/Bag X1, Matieland 7602, South Africa

Received 27 January 2005; received in revised form 18 August 2005; accepted 9 November 2005
Available online 28 November 2005

Abstract

Preparative TREF was used to fractionate 2 commercial LLDPE polymers. These polymers had similar MFI values, density and comonomer content, but differed in comonomer type, 1-butene vs 1-hexene. High resolution solution NMR and solid state NMR was used to characterize the copolymer fractions. Distinct differences in chemical composition distribution could be observed from solution NMR results, and these correlated well with solid state analyses. Conclusions regarding the molecular make-up and crystallization phenomena are made.

Keywords: Polyolefins; High resolution ^{13}C NMR; Fractionation

1. Introduction

The use of preparative TREF to fractionate polyolefins on the basis of crystallizability has received a fair amount of attention in recent years [1–5]. Preparative TREF fractionates ethylene copolymers (LLDPE) on the basis of chemical composition distribution (CCD). This method achieves fractionation on the basis of crystallizability and is mainly influenced by co-monomer content, degree of tacticity (in the case of poly(α-olefins) and monomer sequence length [1,2]. The premise that LLDPE prepared by heterogeneous transition metal catalysts ('Ziegler–Natta catalysts') is in fact a mixture of polymers of different CCD and molecular weights has been shown to be true. We have also had the need to fractionate two commercially available samples of LLDPE in order to elucidate the differences in macroscopic properties of the two materials. These two polymers, prepared by the same catalyst and having nominally similar MFI values, comonomer contents and densities have been shown to have notably different properties, in particular with respect to impact and optical properties. The whole picture is somewhat complicated in that the properties of these materials when used as films are also influenced by the fact that up to 15% of LDPE is normally blended with these polymers during processing [6]. This paper focuses on the use of high resolution NMR (HR NMR) as well as solid state NMR (SS NMR) to fully characterize the fractions obtained by preparative temperature rising fractionation (p-TREF) on two commercial LLDPE samples. One material was a copolymer of ethylene and 1-hexene (LLDPE A) and the other a copolymer of ethylene and 1-butene (LLDPE B). The authors understand that the complex nature of LLDPE polymers produced by heterogeneous transition metal catalysts is well known, this paper deals with the use of alternative techniques for probing the nature of the heterogeneity.

^{13}C HR NMR is a useful technique for determining polymer microstructure. Randall [7] and more recently Rinaldi, et al. [8,9], have demonstrated the wealth of information possible from such an analysis. In particular, Randall and Hsieh have developed models to determine triad sequence distributions and number average sequence lengths. These models have been recently refined by Rinaldi and coworkers to account for the additional peaks observed at 750 MHz [7–9].

Whereas a wealth of knowledge can be obtained from solution NMR, polymers are predominantly used in the solid state, and understanding the properties of solid polymers has been an important factor driving the development of solid state NMR methods. The focus of many of these studies is a molecular level understanding of polymers in their functional

* Corresponding author. Tel.: +27 231 80803168; fax: +27 27 8084967.
E-mail address: ajvr@sun.ac.za (A.J. van Reenen).

0032-3861/$ - see front matter © 2005 Elsevier Ltd. All rights reserved.
doi:10.1016/j.polymer.2005.11.020

state [10]. The resolution of solid state NMR is less than that of solution NMR, but it has been shown that much useful information can be obtained by this technique [11–20]. Solid state NMR provides knowledge of the structure and dynamics of a sample for both crystalline and non-crystalline domains, and even may allow observation of interphase regions.

The raw materials and obtained fractions were characterized by ^{13}C HR NMR, SS NMR and gel permeation chromatography (GPC) to obtain a comprehensive understanding of the structure–property relationship of these polymers, and to see if there is a correlation of the structural information obtained from solution NMR and the SS NMR.

2. Experimental

2.1. Polymers

The samples were commercial copolymers of ethylene-1-butene (LLDPE (C4)) and ethylene-1-hexene (LLDPE (C6)) polymerized in the presence of the same Ziegler–Natta catalyst.

2.2. Preparative temperature rising elution fractionation

Typically, a 2 g polymer sample was dissolved in xylene at 100–130 °C in the presence of a stabilizer to prevent oxidative degradation. The hot polymer solution was then transferred to a heated steel column packed with an inert material (silica gel or washed sand). The polymer was crystallized out of solution onto the inert support material at a rate of 2 °C/h to 25 °C. Polymer fractions were then eluted from the column at temperatures of 40 °C (fraction 1), 68 °C (fraction 2), 85 °C (fraction 3), 95 °C (fraction 4) and 105 °C (fraction 5). For each fraction 300 mL of xylene was used, with the solvent passing through the column at 10 mL/min after allowing 20 min for equilibration at the elution temperature.

2.3. Molecular weight

The molecular weight of the polymers was determined by high temperature gel permeation chromatography (GPC), using a Polymer Labs PL GPC 220. The analysis was performed in 1,2,4-trichlorobenzene (TCB) in the presence of a stabilizer. The columns were calibrated with narrow molecular weight distribution standards of polystyrene and polyethylene.

2.4. High resolution ^{13}C NMR

The solution ^{13}C NMR spectra were obtained at 130 °C on a 500 MHz Varian ^{UNITY}INOVA NMR spectrometer operating at 125 MHz for carbon. A 5 mm PFG switchable/broadband probe (^{1}H–^{19}F, ^{15}N–^{31}P) was used. Typical sample concentrations of the unfractionated polymers were approximately 6 wt% in deuterated tetrachloroethane (*d*-TCE). Sample sizes for the p-TREF fractions ranged from 30–50 mg. Spectra were taken with a 90° flip angle of approximately 6 μs, with continuous proton decoupling, an acquisition time of 1.8 s and a delay time between pulses of 15 s. Under these conditions the spectra are 99% quantitative provided that only the carbon atoms with relaxation delays (T_1) of less than 3 s are taken into account. The number of scans was set to 2400 for the unfractionated polymers and 7200 for the TREF fractions. Spectra were obtained with either a S/N of 5000 (based on the main backbone methylene carbon resonance) or a minimum number of scans equal to 2400 (7200), which ever came first. Hence, the analysis time ranged from 3 to 10 h. The chemical shifts were referenced internally to the main backbone methylene carbon resonance (30 ppm). The comonomer content, triad sequence distribution and number average sequence length distribution were determined according to the literature procedures [7–9].

2.5. Solid state NMR

The solid state NMR experiments were carried out on a 400 MHz Varian ^{UNITY}INOVA NMR spectrometer. The ^{13}C spectra were obtained under dipolar decoupling, and all experiments were carried out with magic angle spinning in either 7.5 mm (unfractionated polymers) or 4 mm (TREF fractions) zirconia rotors at a spinning speed of 3.5 or 7 kHz, respectively. CP-MAS experiments were performed using a 90° pulse width of 4 μs. The contact times for cross-polarization was 1 ms. Spin-lattice relaxation times (T_1) were determined using an inversion recovery cross polarization pulse program. Relaxation delays of up to 5000 s were used to ensure full recovery of the equilibrium magnetization for the crystalline phase. All samples were analyzed in exactly the same manner for comparison purposes. Adamantane was used as an external chemical shift standard (upfield peak set at 29.5 ppm).

2.6. Nomenclature and structure

The nomenclature used for assigning the polymer backbone and side-chain carbons discriminated by ^{13}C NMR spectroscopy is depicted in Scheme 1.

The distinguishable backbone carbons are designated by Greek symbols, while the side-chain carbons are numbered consecutively, starting with the methyl group and ending with the methylene carbon (carbon '4' in this example) bonded to the polymer backbone. This is the nomenclature used by Randall

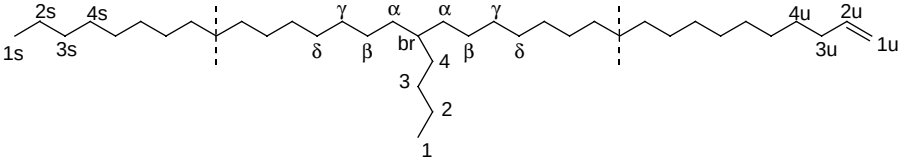

Scheme 1. Assignment of polymer backbone and side-chain carbons.

Table 1
Characteristics of p-TREF fractions

Sample	Fraction	Elution T (°C)	Mass (%)	M_w	M_n	M_w/M_n
LLDPE (C4)	B1	40	14.96	193,454	40,334	4.8
	B2	68	29.04	233,832	66,077	3.5
	B3	85	32.79	275,245	91,899	3.0
	B4	95	22.87	329,827	131,678	2.5
	B5	105	0.34	–	–	–
LLDPE (C6)	A1	40	15.38	121,594	31,274	3.9
	A2	68	21.96	167,695	49,755	3.4
	A3	85	27.08	272,339	85,705	3.2
	A4	95	27.00	365,143	130,263	2.8
	A5	105	8.58	340,047	125,764	2.7

[21] and De Pooter et al., [22]. The branch point is designated by the carbon labeled 'br' and is used to determine the comonomer content in the polymer (can be easily isolated). Two of the carbons from the comonomer reside in the backbone. Therefore, the number of branched carbons is multiplied by two in Eq. (1) below. The saturated end group carbons in the main chain are designated by 1s ,2s and 3s starting at the methyl carbon at the chain end as position '1'. The unsaturated end groups are correspondingly labeled 1u, 2u, and 3u.

$$\text{Comonomer (Mol\%)} = \frac{2\int \text{Branched C's}}{\sum\int \text{Backbone C's}} \times 100 \quad (1)$$

3. Results

3.1. HR NMR

Molecular weight data for the fractions obtained by p-TREF for copolymers A and B are represented in Table 1.

Table 1 shows the general tendency of the molecular weight increasing with increasing elution temperature, which was expected [23]. The decrease in molecular weight distribution with elution temperature is also expected, since fractionation is based on chemical composition. For LLDPE (C6), the fractions eluting at higher temperatures comprises most of the weight while for LLDPE (C4) the weight tend to lie toward the fractions eluting at lower temperatures. LLDPE (C6) contains a significant amount of fraction 5, while only a small amount of this fraction was collected for LLDPE (C4).

Copolymer composition, triad distribution and number average sequence length (n_E) were obtained from solution ^{13}C NMR. A spectrum of LLDPE (C6) fraction A1 is shown in Fig. 1 to illustrate the chemical shift assignments and the wealth of information possible from the analysis. Figs. 2 and 3 show the stacked plots for the fractions of both LLDPE (C4) and LLDPE (C6).

Table 2 shows the triad sequence distributions for the raw materials and fractions where E (ethylene), H (1-hexene) and B (1-butene) represent the repeat unit, for example the triad [EEE] represents three consecutive ethylene units along the backbone while [EHE] refers to an isolated branch. The unfractionated polymers appear to have similar comonomer contents. However, the distribution of comonomer along

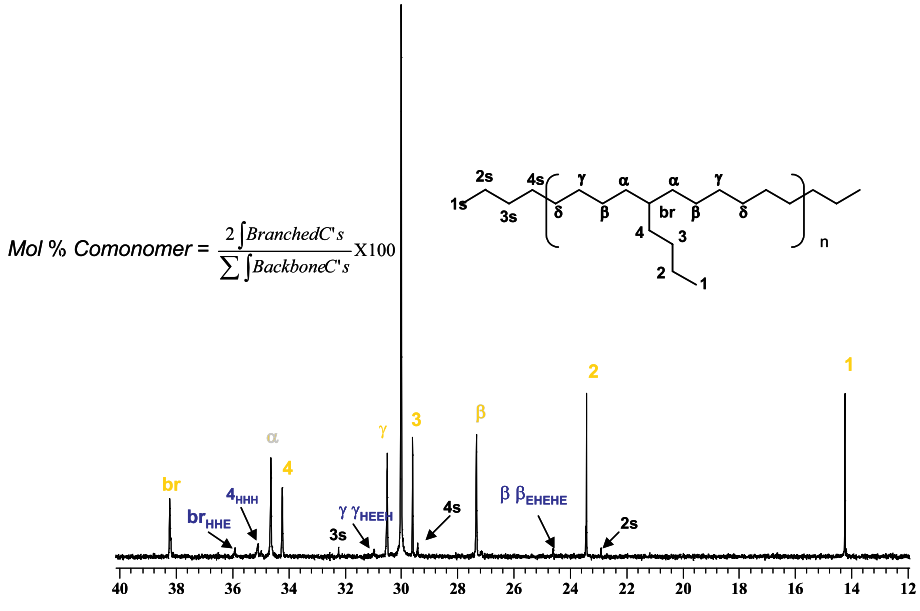

Fig. 1. ^{13}C NMR spectrum of LLDPE (C6) fraction A1, containing 10.5 mol% 1-hexene.

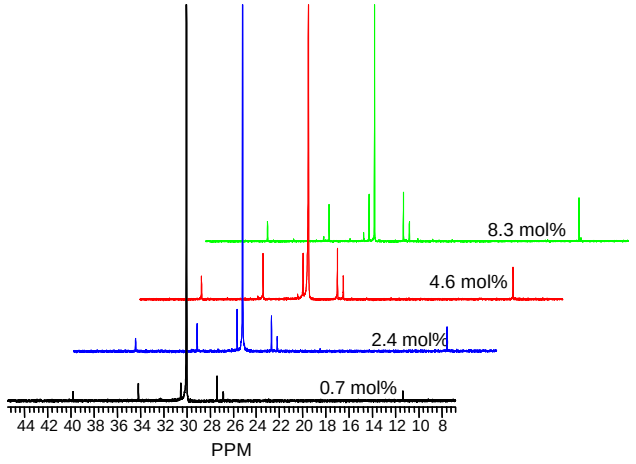

Fig. 2. Stacked plot of ^{13}C NMR spectra for the fractions of LLDPE (C4) with various mol% of 1-butene.

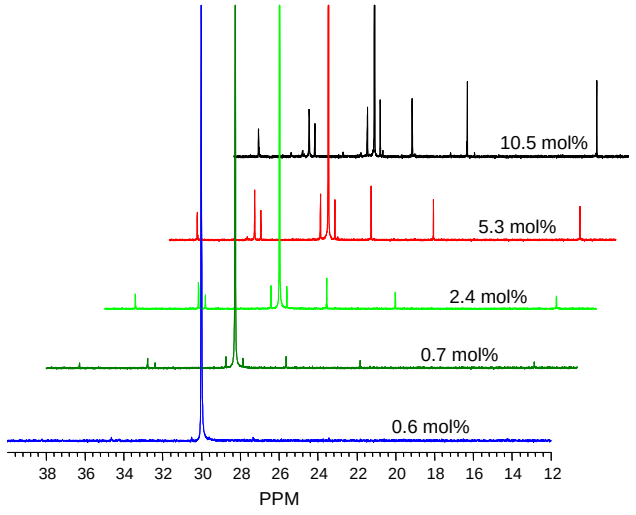

Fig. 3. Stacked plot of ^{13}C NMR spectra for the fractions of LLDPE (C6) with various mol% of 1-hexene.

the backbone is different for the two polymers. This is evident upon inspection of the fractions. Fraction B1 (LLDPE (C4)) and A1 (LLDPE (C6)) are significantly different with A1 having a higher degree of short chain branches (SCB) per chain than B1. This is demonstrated by the significantly lower [EEE] sequences present in A1 as well as by the increased amount of cluster sequences, [EHH] and [HEH]. In addition fractions A2 and A3 also show some clustering which is not observed for the LLDPE (C4) fractions, B2 and B3.

The sample size of fraction B5 was too small for analysis (4 mg, 0.3 wt% of total sample). Fraction A5 on the other hand makes up almost 9% of the total weight of the unfractionated LLDPE (C6). This is a significant amount when one considers that its microstructure is very similar to fraction A4 (compare fraction B4) with the only noteworthy difference being the number average sequence length. A4 and A5 together comprise ~36 wt% of LLDPE (C6), while B4 (and B5) only make up ~24% of the weight of LLDPE (C4). Thus, LLDPE (C6) contains a considerable amount of almost linear polyethylene chains which could have a significant effect on its crystallization behavior.

3.2. SS NMR

Solid state NMR experiments included ^{13}C T_1 determination using an inversion recovery pulse sequence with cross-polarization and magic angle spinning. The experiment time was typically 36 h per sample. Relaxation times of up to 5000 s were used to ensure complete recovery of the crystalline (rigid) signal over the time interval. One of the reviewers alerted us to the fact that this is a very time consuming experiment and probably not the most effective for industrial purposes. Other experiments such as ^{1}H-FID (for determination of the amount of crystalline, amorphous and interphase components) and spin diffusion (for average crystallite size determination) may be used for faster results.

The calculations of the mass fractions were done by least squares line fittings using the software program Origin 7.0. The total ^{13}C NMR signal intensity (25–40 ppm) was decomposed into two or three peaks with 100% Lorentzian line shape. A three-component fit was shown to be superior to a two-component fit for every sample. This is evident in the excellent correlations achieved between the experimental data and the calculated values as illustrated by the R^2 value of 0.999 and the

Table 2
Triad sequence distributions for LLDPE (C4) and LLDPE (C6)

Sample	Fraction	Mol% [**B**]	[BBB]	[EBB]	[EBE]	[BEB]	[BEE]	[EEE]	n_E
LLDPE (C4)	Pellets	3.0	0.0	0.0	3.0	0.0	5.9	91.1	33.0
	B1	8.3	0.0	0.9	7.4	0.8	16.5	74.4	12
	B2	4.6	0.0	0.0	4.6	0.0	9.0	86.4	21
	B3	2.4	0.0	0.0	2.4	0.0	4.9	92.7	40
	B4	0.7	0.0	0.0	0.7	0.0	1.5	97.7	135
Sample	Fraction	Mol% [**H**]	[HHH]	[EHH]	[EHE]	[HEH]	[HEE]	[EEE]	n_E
LLDPE (C6)	Pellets	3.1	0.0	0.3	2.8	0.4	9.4	87.1	33.0
	A1	10.5	0.0	1.5	8.9	1.5	26.6	61.5	9.0
	A2	5.3	0.0	0.4	4.9	0.4	14.7	79.7	19.0
	A3	2.7	0.0	0.1	2.3	0.4	7.2	90.1	42.0
	A4	0.7	0.0	0.0	0.7	0.0	2.5	96.8	143
	A5	0.6	0.0	0.0	0.6	0.0	2.2	97.2	180

B and **H** refer to the comonomer units 1-butene and 1-hexene respectively.

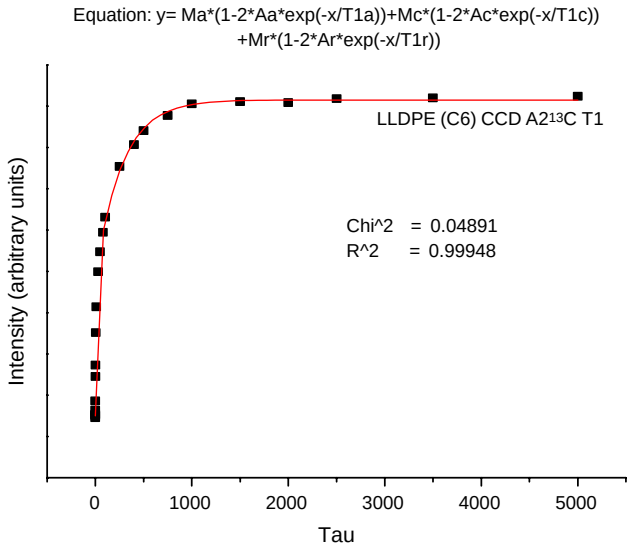

Fig. 4. Example of a three component fit to the ^{13}C T_1 data obtained for fraction A2.

very low χ^2 obtained for the three-component model in each case. Fig. 4 shows the three component fit to the experimental data for fraction A2.

In the equation in Fig. 4, it was found that an improved fit was attained only when the constant A was included in the model. This A factor scales with the magnetization contribution for each component. It is thought to be a compensation factor for incomplete recovery of the equilibrium magnetization. Three significantly different spin-lattice relaxation times (T_1's) were identified (Table 3). These were correlated to a fast relaxing component (amorphous), an intermediate relaxing component (termed here rigid amorphous) and a slow relaxing component (crystalline).

The contributions from each of these components were determined from the ratio of the pre-exponential factors (in each case the product of A_x and M_x). Thus, the result of the fit could not be easily manipulated. The same results were obtained irrespective of the starting values chosen for the model. The results are represented in Table 4 below.

Table 3
T_1 data, obtained from the equation in Fig. 4, for the unfractionated raw material and p-TREF fractions

Sample	Fraction	^{13}C T_{1c} (s)	^{13}C T_{1a} (s)	^{13}C T_{1r} (s)
LLDPE (C4)	Pellets	199 (16)	0.59 (0.13)	16 (5)
	B1	297 (33)	0.27 (0.08)	19 (4)
	B2	268 (33)	0.28 (0.19)	16 (5)
	B3	346 (36)	0.76 (0.19)	36 (12)
	B4	431 (50)	1.03 (0.43)	41 (17)
LLDPE (C6)	Pellets	250 (18)	0.49 (0.09)	25 (4)
	A1	249 (35)	0.43 (0.12)	18 (5)
	A2	274 (14)	0.37 (0.13)	12 (2)
	A3	367 (25)	0.79 (0.15)	34 (7)
	A4	457 (40)	0.86 (0.25)	51(13)
	A5	318 (23)	0.10 (0.07)	19 (4)

Note: standard deviations in parenthesis.

Table 4
Contributions from fast, intermediate and slow relaxing components as determined from the equation in Fig. 4, for the unfractionated raw material and p-TREF fractions

Sample	Fraction	Crystallinity (%)	Amorphous (%)	Rigid amorphous (%)
LLDPE (C4)	Pellets	53.1	24.4	22.5
	B1	43.7	24.5	31.9
	B2	54.1	16.4	29.5
	B3	54.3	18.8	26.9
	B4	61.5	13.7	24.8
LLDPE (C6)	Pellets	47.7	20.3	32.1
	A1	39.7	26.9	33.4
	A2	56.1	15.3	28.6
	A3	54.7	17.1	28.2
	A4	61.2	13.1	25.7
	A5	65.0	7.5	27.4

The T_1 values of the crystalline domain can be correlated to crystallite size and perfection [24]. The fractions of each polymer represent a group of polymers with varying branch content only. In such samples the crystallite thickness will be determined primarily by the distribution of structural irregularities (branches) along the polymer backbone. Thus, it makes sense that a decrease in comonomer content will result in an increase in crystallite thickness, because of the relationship between extended chain length and crystallite thickness. The general increase in T_{1c} from fraction A1 to A5 and B1 to B5 is therefore as expected. If one considers this carefully, it makes sense then that for the same volume, the percentage rigid amorphous will decrease, since bigger crystallites will have fewer interfaces than smaller crystallites occupying the same space. This is indeed observed in the data in Table 4. The anomalous behavior of fraction A5 is evident in all the data throughout.

The behavior of increasing crystallinity with elution temperature (B1–B4 and A1–A5) is expected as TREF separates using differences in crystallizability according to chemical composition distribution. This is indeed observed in the ^{13}C CP-MAS spectra in Figs. 5 and 6. Polyethylene and copolymers thereof exist in the all-trans conformation in the crystalline phase. The chemical shifts observed in the spectra for the crystalline and amorphous phases are in accord with the γ-*gauche* effect where the presence of methylene bonds in the gauche conformation cause an upfield shift of up to 5 ppm [10]. The CP-MAS experiment favors methylene groups in rigid environments since magnetization transfer is more effective in these regions, therefore an increase in the crystalline peak intensity for the various fractions can be attributed to an increase in crystallinity.

Table 5 indicates the contributions from the various fractions to the determination of the crystallinity of the raw material. There is good agreement between the crystallinity calculated from the various fractions to that determined for the

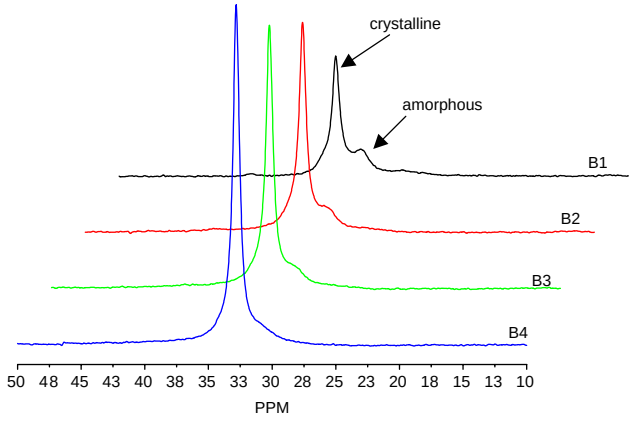

Fig. 5. ^{13}C CP MAS spectra of LLDPE (C4) fractions B1 to B4.

raw material for LLDPE (C4). For LLDPE (C6) however, the crystallinity is significantly lower than the weighted average crystallinity calculated from the fractions. The reason is thought to lie in the collective effect of the higher degree of SCB's and cluster sequences present in the lower molecular weight fractions of LLDPE (C6) as well as the predominantly linear high molecular weight fractions and its influence on the crystallization behavior of the total sample.

It will be seen that the T_{1c} value found for the unfractionated polymer is not the average calculated from the T_{1c}-values for the individual weight fractions. This can be ascribed to the dependence of T_{1c} on the crystallite size and not the degree of crystallinity [24,25]. In this regard, e.g. fraction A2 and A3 have similar percent crystallinities but their T_{1c}'s are significantly different. The disparity in the T_{1c}'s can be ascribed to different morphologies of the two samples evidenced by two crystallization peaks observed in the TREF profile for fraction A2 versus one for fraction A3.

Furthermore, in an unfractionated polymer (raw material), the heterogeneous chains are allowed to 'co-crystallize', thus leading to crystallites of average size because of the varying distribution of comonomer along the backbone. In contrast, when these chains are separated into various fractions

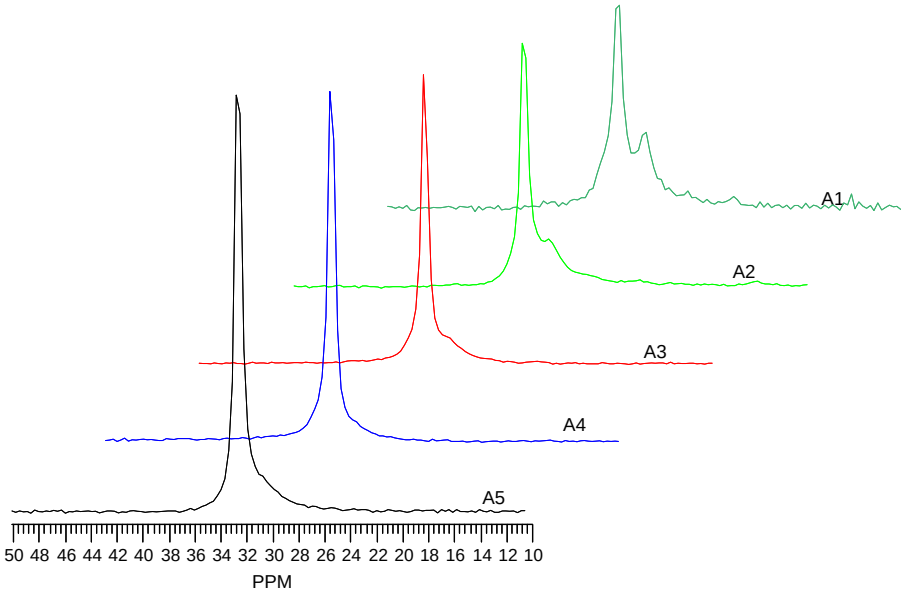

Fig. 6. ^{13}C CP MAS spectra of LLDPE (C6) fractions A1 to A5.

Table 5
Crystallinity contributions from each fraction

Sample	Fraction	T_{1c} (s)	Crystallinity (%)	Weight fraction (%)	Crystallinity contributions from each fraction	T_{1c} contributions from fractions
LLDPE (C4)	Pellets	199.0	53.1	1	54.3	336
	B1	297.0	43.7	0.15	6.6	44.5
	B2	268.0	54.1	0.29	15.7	77.7
	B3	346.0	54.3	0.33	17.9	114.2
	B4	431.0	61.5	0.23	14.1	99.1
LLDPE (C6)	Pellets	250.0	47.7	1	55.4	349
	A1	249.0	39.7	0.15	6.0	37.4
	A2	274.0	56.1	0.22	12.3	60.3
	A3	367.0	54.7	0.27	14.8	99.1
	A4	457.0	61.2	0.27	16.5	123.4
	A5	318.0	65.0	0.09	5.85	28.6

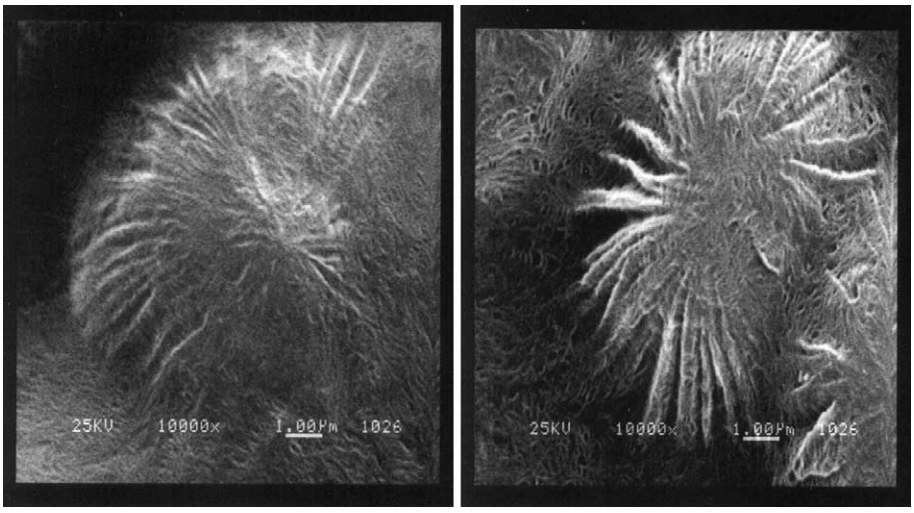

Fig. 7. SEM micrographs[2] of etched polymer surfaces for LLDPE (C4) (left) and LLDPE (C6) (right).

according to their branching distribution, the crystallite size for each fraction will be representative of all the chains present in that fraction, hence a more homogenous distribution of crystallite sizes and therefore the discrepancy in the T_{1c} calculated from the fractions and that determined experimentally for the total sample.

On the whole, it was observed that the crystalline T_1's for LLDPE (C4) were less than that for LLDPE (C6). It was previously reported that shorter crystalline T_1's were found for samples which had the same content as the other samples but a more homogenous distribution of SCB's along the backbone [24]. This is in agreement with the results reported in our work. The solution NMR results alluded to LLDPE (C6) being a more heterogeneous polymer than LLDPE (C4). This has been further substantiated in the solid state data observed for these two samples. The increased heterogeneity in the microstructure of LLDPE (C6) when compared to LLDPE (C4) is also evident in Fig. 7 which shows the SEM micrographs of the spherulitic structure of the two polymers. The structure for LLDPE (C6) appears to be fibrous and non-uniform when compared to LLDPE (C4).

4. Conclusions

Preparative TREF in conjunction with NMR can provide us with a wealth of information and insight into the microstructure of a polymer that can otherwise not be obtained. In this study ethylene-*co*-1-butene and ethylene-*co*-1-hexene had very similar densities, MFI's, comonomer (mol%) contents and percentage crystallinity; however distinct differences were observed in the physical properties of these two polymers. LLDPE (C6) could be fractionated into five fractions, while only four significant fractions were obtained for LLDPE (C4). The fraction that eluted at the highest temperature for LLDPE (C6) comprised 9% of the total weight of the polymer. The observed differences could therefore be ascribed to increased heterogeneity of the polymer chains of the ethylene-1-hexene copolymer as was illustrated by ^{13}C NMR.

Although the amount of crystallinity was the same for both polymers, the type of crystallinity differed significantly. It is believed that the higher degree of clustering in LLDPE (C6) inhibits crystallization more and thereby increases the number of tie-molecules in the polymer, making it a stronger product. Hence, the higher impact strength observed for LLDPE (C6) over LLDPE (C4). This was further substantiated by the coarser spherulitic structure of LLDPE (C6) observed in the SEM micrographs. This, in addition to the fact that LLDPE (C6) contains a higher amount of linear chains that can crystallize at higher temperatures, thereby forming larger crystals, explains the poor optical properties of the material. The results from triad sequence distributions, relaxation studies, crystallization and melting behavior all point to LLDPE (C6) having a more heterogeneous distribution of short chain branches along the backbone than LLDPE (C4) which in turn has significant effects on the observed properties.

References

[1] Wild L. Adv Polym Sci 1990;98:1–67.
[2] Junting X, Linxian F. Eur Pol J 2000;36:867–78.
[3] Chem F, Shanks RA, Amarasinghe G. Polymer 2001;42:4579–87.
[4] Mierau U, Voigt D, Bohme F, Brauer E. J Appl Polym Sci 1997;63:283–8.
[5] Pires M, Mauber RS, Liberman SA. J Appl Polym Sci 2004;92:2155–62.
[6] Guichon O, Séguéla R, David L, Vigier G. J Polym Sci, Polym Phys Ed 2003;41:327–40.
[7] Hsieh ET, Randall JC. Macromolecules 1982;15:353–60.
[8] Liu W, Rinaldi PL, McIntosh LH, Quirk RP. Macromolecules 2001;34: 4757–67.
[9] Sahoo SK, Zhang T, Reddy DV, Rinaldi PL, McIntosh LH, Quirk RP. Macromolecules 2003;36:4017–28.
[10] Bovey FA, Mirau PA. NMR of polymers. New York: Academic Press, Inc; 1996 [chapter 4].
[11] Tonelli A. NMR spectroscopy and polymer microstructure: the conformational connection. New York: VCH; 1989.
[12] VanderHart DL, Earl WL, Garroway AN. J Magn Reson 1981;44: 361–401.

[13] Mathias LJ. Solid state NMR of polymers. New York: Plenum; 1991.
[14] Hu W-G, Boeffel C, Schmidt-Rohr K. Macromolecules 1999;32:1611–9.
[15] Hu W, Srivatsan S, Sirota EB. Macromolecules 2002;35:5013–24.
[16] Kuwabara K, Hironori K, Tsuji M, Horii F. Macromolecules 2000;33: 7093–100.
[17] De Langen M, Prins KO. Polymer 2000;41(3):1175–82.
[18] Hu W-G, Schmidt-Rohr K. Polymer 2000;41(8):2979–87.
[19] Schmidt-Rohr K, Spiess HW. Macromolecules 1991;24:5288–93.
[20] Alamo RG, Blanco JA, Carrilero I, Fu R. Polymer 2002;43:1857–65.
[21] Woodward AE. In: Bovey FA, editor. Polymer characterization by ESR and NMR. Washington, DC: American Chemical Society; 1980. p. 94–118 [chapter 6].
[22] De Pooter M, Smith PB, Dohrer KK, Bennett KF, Meadows MD, Smith CG, et al. J Appl Polym Sci 1991;42:399–408.
[23] Galland GB, Mauler RS, Da Silva LP, Liberman S, Da Silva Filho AA, Quijada R. J Appl Polym Sci 2002;84:155–63.
[24] Axelson DE. J Polym Sci, Polym Phys Ed 1983;21:2319–35.
[25] Axelson DE. J Polym Sci, Polym Phys Ed 1982;20:1427–35.